The 2017 World Congress on
Advances in Structural Engineering and Mechanics (ASEM17)
28 August - 1 September, 2017, Ilsan(Seoul), Korea

A Study on Effective Properties of Heterogeneous Representative Volume Element under Various Boundary Conditions

*Sungwoo Jeong[1)], Hyungjun Lim[1)], Fei-Yan Zhu[1)] and Gunjin Yun[2)]

[1), 2)] *Department of Mechanical & Aerospace Engineering, Seoul National University, Seoul, Korea*
[2)] *gunjin.yun@snu.ac.kr*

ABSTRACT

This paper reports variability of effective elastic properties of a heterogeneous representative volume element (RVE) under displacement, traction and periodic boundary conditions. Effective stiffnesses of the heterogeneous RVE were obtained by finite element-based computational asymptotic homogenization method under three different boundary conditions. In addition, effects of spatial random distributions of matrix properties were also investigated. Varying effective stiffnesses with RVE heterogeneities are for micromechanics inverse characterization of constituents.

1. INTRODUCTION

Multiscale modeling and analysis have become a common engineering tool for design of advanced composite materials since not only does it allow design of microstructure but also predict root flaws that may lead to failure of structures. One of the key steps in the multiscale analyses of composite materials is the homogenization that can bridge multiscale models through effective properties. The effective properties of representative volume element (RVE) are affected by size of RVE, volume fraction, stiffness contrast of constituents, random geometry of the composite constituents, boundary conditions, etc. Typically, the effective stiffness is overestimated under displacement boundary conditions whereas underestimated under traction boundary conditions as provided by Voigt-Reuss and Hashin-Shtrikman theoretical bounds (Hashin and Shtrikman 1963). For RVEs having periodic microstructure, periodic boundary condition provides intermediate effective stiffness and shows faster convergence toward the effective stiffness as the RVE size increases.

In addition to the boundary condition effects, the effective stiffness errors are also associated with stiffness contrast and geometry of the composite constituents, etc. (Hollister and Kikuehi 1992). According to Terada, et al.(Terada, Hori et al. 2000), as

---

[1)] Graduate students
[2)] Corresponding author, Associate Professor, Gwanak-gu Gwanak-ro 1 Building 301 Room 1308, Seoul, South Korea, 08826, Tel)+82-2-880-8302, Fax)+82-2-887-2662, email)gunjin.yun@snu.ac.kr

long as the size of RVE is large enough under periodic boundary conditions, the effective stiffness of geometrically heterogeneous RVEs are reliably estimated by FE-based computational asymptotic homogenization method. The morphology and random distribution of constituents' properties are known as the most influential factors to the effective properties of composite materials (Salnikov, Lemaitre et al. 2015). Zhou *et al.* recently considered randomness of constituents' material properties to quantify variability in the overall elastic properties of composite materials (Zhou, Gosling et al. 2016). Variability of effective properties was compared for different homogenization methods such as Mori-Tanaka(Mori and Tanaka 1973), vanishing fiber diameter(Dvorak and Baheieldin 1982) and self-consistent method (Hill 1965) and two FEM-based cell methods by using a stochastic perturbation technique (Kaminski and Pawlak 2015). Although geometrical heterogeneity has been considered by researchers (Stefanou, Savvas et al. 2015), the spatial random distribution of material properties have not been studied in correlation with the RVE size. Spatial random distributions of matrix properties are due to uncertainty in chemical reactions around the matrix-fiber interface, random fiber-packing, and heterogeneous matrix-dominated stiffness reduction by damage evolutions under in-service mechanical and environmental loadings. The spatial randomness of matrix properties at the microscale has become even more significant in polymer nanocomposites which have non-uniform dispersion and distributions of nano-fillers (Spanos and Kontsos 2008).

Numerous analytical (Hill 1965, Mori and Tanaka 1973, Benssousan, Lions et al. 1978) and computational homogenization methods (Nguyen, Stroeven et al. 2011, Zhuang, Wang et al. 2015) have been proposed in the past for linear(Zhuang, Wang et al. 2015), nonlinear(Zhu, Wang et al.) and even the multi-physics problems(Ozdemir, Brekelmans et al. 2008). The analytical homogenization methods based on the Eshelby inclusion solution (Eshelby 1957) are limited to linear materials and simple ellipsoidal inclusions. On the contrary, the computational homogenization method is applicable to any complex microstructure and even nonlinear problems. A Fast Fourier Transform(FFT)-based homogenization method was proposed as a computationally efficient approach (Salnikov, Lemaitre et al. 2015). In this study, a FE-based computational homogenization method (Yuan and Fish 2008) is adopted for obtaining effective properties of heterogeneous RVE.

In this paper, effects of boundary conditions and spatial random distributions of constituents' properties on the effective properties were investigated. In Section 2, theoretical backgrounds and boundary conditions are revisited. It is followed by random field modeling and computational homogenization technique in Section 3 and 4, respectively. Results are discussed in Section 5. Finally, conclusions are summarized in Section 6.

2. EFFECTS OF BOUNDARY CONDITIONS

The RVE is defined as a volume that has effective stiffness invariant to boundary conditions. For a volume element smaller than the RVE, the effective stiffness is affected by the boundary conditions. Therefore, they are distinguished from the effective stiffness by the name of apparent stiffness. The volume giving the apparent stiffness is named as an "apparent RVE" herein. The window size is defined as a ratio of edge length (L) of RVE to characteristic length (d) of inclusions, which is δ=L/d >>1. For an apparent RVE, the apparent stiffness under displacement boundary conditions converge to the effective stiffness from upper bounds as the window size increases. On the contrary, the apparent stiffness under traction boundary conditions converge to the effective stiffness from lower bounds as the window size increases. Voigt and Reuss bounds provide the theoretical upper and lower bounds, respectively.

Under the homogeneous boundary conditions, the volume average stress($\bar{\sigma}_{ij}$) and strain($\bar{\varepsilon}_{ij}$) are related by Hookes' law,

$$\bar{\sigma}_{ij} = C^{eff}_{ijkl}\bar{\varepsilon}_{kl} \quad \text{and} \quad \bar{\varepsilon}_{ij} = S^{eff}_{ijkl}\bar{\sigma}_{kl} \tag{1}$$

where C^{eff}_{ijkl} are the effective elastic moduli and S^{eff}_{ijkl} are the effective elastic compliances. By the average stress and strain theorem, the average stress and strain are identical to the homogeneous boundary stress(σ^0_{ij}) and strain(ε^0_{ij}), respectively as long as inclusions are perfectly bonded to the matrix.

Applying the average strain theorem, the displacement boundary condition (DBC) can be expressed as

$$u_i(\Gamma) = \varepsilon^0_{ij}x_j, \quad \forall x_j \in \Gamma \tag{2}$$

where ε^0_{ij} is a uniform strain that is independent with a location x_j; and Γ is the surface boundary.

Applying the average stress theorem, the traction boundary condition (TBC) can be expressed as

$$t_i(\Gamma) = \sigma^0_{ij}n_j, \quad \forall x_j \in \Gamma \tag{3}$$

Where σ^0_{ij} is a uniform stress that is independent with x_j; the vector normal to Γ at x_j is denoted by n_j; and t_i is the traction. Under both DBC and TBC, "unit" strain or stress can be applied component-by-component to the RVE and corresponding stresses or strains become stiffness and compliances, respectively.

The periodic boundary condition (PBC) can also be used to determine the effective stiffnesses. The PBC can be expressed as

$$u_i(x_1, x_2, x_3) = u^*_i(x_1, x_2, x_3) + \varepsilon^0_{ij}x_j \qquad t_i(x_1, x_2, x_3) = -t^*_i(x_1, x_2, x_3) \tag{4}$$

ε^0_{ij} is the average strain of periodic structure and the u_i and u^*_i are displacement components at corresponding points on the facing surfaces. t_i and t^*_i are traction components.

As aforementioned, the effective stiffnesses for apparent RVE take hierarchical bounds as

$$\mathrm{C}^{\mathrm{R}} \le \left(S^{app}_t\right)^{-1} \le \left(S^{eff}_t\right)^{-1} \le C^{eff} \le C^{eff}_d \le C^{app}_d \le C^V \tag{5}$$

where C^{R} and C^V are Reuss and Voigt bounds; the superscript "app" means apparent stiffness and compliance; the subscript "d" and "t" indicate DBC and TBC, respectively.

3. EFFECTS OF SPATIAL RANDOM DISTRIBUTIONS OF RVE PROPERTIES

As aforementioned, matrix properties could show non-uniform distributions within RVE. Their infinite dimension in the probability space can be reduced to finite dimensions by three-dimensional Karhunen-Loève (KL) expansion method.

The KL expansion decomposes a spatial random field $\boldsymbol{H(x,y,z)}$ to a deterministic and a stochastic part as follows

$$\boldsymbol{H(x,y,z)} = \boldsymbol{< H >} + \boldsymbol{\sum_{i=1}^{m} \sqrt{\lambda_i}\, \varphi_i[\xi_i]} \tag{6}$$

where $< H >$ is the mean value, ξ is the normal variable, λ_i, φ_i are the eigenvalue and eigenvector of an analytical covariance kernel, respectively. The solution of Fredholm integral equation is λ_i, φ_i

$$\boldsymbol{\int_{\Omega_{2e}} C(\vec{X}_1, \vec{X}_2)\, \varphi_k(\vec{X}_2) dV_{2e} = \lambda_k \varphi_k(\vec{X}_1)} \tag{7}$$

In the Fredholm integral equation, $\boldsymbol{C(\vec{X}_1, \vec{X}_2)}$ is a covariance function that takes an exponential form:

$$\boldsymbol{C(\vec{X_1}, \vec{X_2}) = \sigma^2 exp(-\frac{|x_1 - x_2|}{L_x} - \frac{|y_1 - y_2|}{L_y} - \frac{|z_1 - z_2|}{L_z})} \tag{8}$$

Where $\boldsymbol{\vec{X}_1(x_1, y_1, z_1)}$ and $\boldsymbol{\vec{X}_2(x_2, y_2, z_2)}$ are randomly selected two points in the domains; σ^2 is the variation; and L_i is the correlation length in *i*th direction. Galerkin finite element method was used to discretize the KL eigenfunctions.

4. FE-BASED COMPUTATIONAL HOMOGENIZATION METHOD

There are six loading cases where one of the coarse-scale strains is unit with zero for the rest of other strains. Then the homogenized linear elastic constitutive tensor components are given as

$$^{d}C_{ijmn}^{eff} = \frac{1}{|\Theta|}\int_{\Theta} {}^{d}\sigma_{ij}^{mn} d\Theta = \frac{1}{|\Theta|}\int_{\Theta} C_{ijkl}(\frac{\partial\, {}^{d}\chi_k^{mn}}{\partial y_l} + I_{klmn}) d\Theta \tag{9}$$

Where $^{d}\chi_k^{mn}$ is the displacement influence function under the course-scale strain (i.e. displacement) boundary conditions ($\varepsilon_{mn}^{c} = 1$) and $I_{klmn} = 0.5(\delta_{mk}\delta_{nl} + \delta_{nk}\delta_{ml})$ is the fourth-order symmetric tensor. The stress influence function $^{d}\sigma_{ij}^{mn}$ are stresses σ_{ij} generated by subjecting the RVE to a unit coarse-scale strain $\varepsilon_{mn}^{c} = 1$. When the six loading cases of the coarse-scale stress (i.e. traction) boundary conditions($\sigma_{mn}^{c} = 1$) are applied, the homogenized linear elastic compliance tensor components are given as

$$^{t}S_{ijmn}^{eff} = \frac{1}{|\Theta|}\int_{\Theta} {}^{t}\varepsilon_{ij}^{mn} d\Theta = \frac{1}{|\Theta|}\int_{\Theta} S_{ijkl}(\, {}^{t}\psi_{kl}^{mn} + I_{klmn}) d\Theta \tag{10}$$

where $^{t}\psi_{kl}^{mn}$ is the stress influence function under $\sigma_{mn}^{c} = 1$, which transforms coarse-scale stress fields to fine-scale stress fields. The strain influence function $^{t}\varepsilon_{ij}^{mn}$ are strains ε_{ij} generated by subjecting the RVE to a unit coarse-scale stress $\sigma_{mn}^{c} = 1$. The effective stiffness and compliances in Eq. (9) and (10) are computed numerically as follows

$$ {}^{d}C_{ijmn}^{eff} = \frac{1}{|\Theta|}\sum_{I=1}^{N_{int}} {}^{d}\sigma_{ij}^{mn}(y_I)J(y_I)W(y_I) \tag{11} $$

Where $\mathrm{N_{int}}$ is the total number of integration points; J and W are the Jacobian and weighting factor, respectively. Similarly, the homogenized effective compliance tensor under coarse-scale traction boundary conditions is computed as

$$ {}^{t}S_{ijmn}^{eff} = \frac{1}{|\Theta|}\sum_{I=1}^{N_{int}} {}^{t}\varepsilon_{ij}^{mn}(y_I)J(y_I)W(y_I) \tag{12} $$

It is known that ${}^{d}C_{ijmn}^{eff} \neq \left({}^{t}S_{ijmn}^{eff}\right)^{-1}$ for heterogeneous RVE while they are identical for homogeneous RVE (Ostoja-Starzewski 2008). Therefore, the extents of the difference are measured by deviation of the product $\left({}^{t}S_{ijmn}^{eff}\right)^{-1} : {}^{d}C_{ijmn}^{eff}$ from unity.

5. NUMERICAL RESULTS AND DISCUSSIONS

A simple RVE of AS4/3501-6 with volume fraction 0.6 having single unidirectional fiber within matrix was built as an example (Fig 1). Eight-node brick finite elements from a verified in-house code were used for the model. Diameter of the fiber is 7 μm and the RVE is a cube of length 8 μm. Total 840 elements were used for matrix and 1040 for fibers. For simplification of cases, both fiber and matrix are assumed as an isotropic linear elastic material.

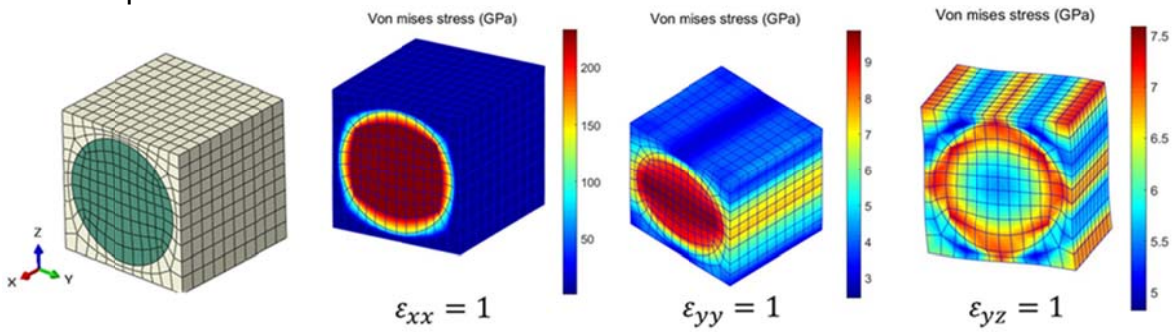

Fig. 1 RVE and von Mises stress contour of three different loading case

Table 1 shows comparison results of experimental data with present homogenization results.

Table 1 Comparisons of homogenized effective stiffnesses

	$\mathrm{E_1}(GPa)$	$\mathrm{E_2}(GPa)$	$\mathrm{G_{12}}(GPa)$	$\mathrm{G_{23}}(GPa)$	ν_{12}	ν_{23}
AS4	235.0	14.0	28.0	8.74	0.2	0.25
3501-6	4.8	4.8	1.8	1.8	0.34	0.34
AS4/3501-6 ($\mathrm{v_f} = 0.6$)	142.6	9.6	6.0	3.1	0.25	0.35
Experiment (Sun and Vaidya 1996)	142.0	10.3	7.6	3.8	-	-
Present	142.02	9.59	6.038	3.57	0.253	0.350

5.1 Effects of Boundary Conditions and Stiffness Contrast Between Phases

The stiffness ratios of matrix to fiber were varied by setting E_f= 5GPa and E_m= 5, 4.25, 3.75, 2.5, 1.25, 0.5, 0.05 (GPa). Fig. 1 shows comparisons of effective engineering constants for different boundary conditions and effects of stiffness contrast between the constituents. For homogeneous materials, there effective stiffnesses were identical for TBC, DBC and PBC. Except G_{12}, effective stiffnesses from PBC were closer to those from DBC since PBC is based on displacement boundary conditions.

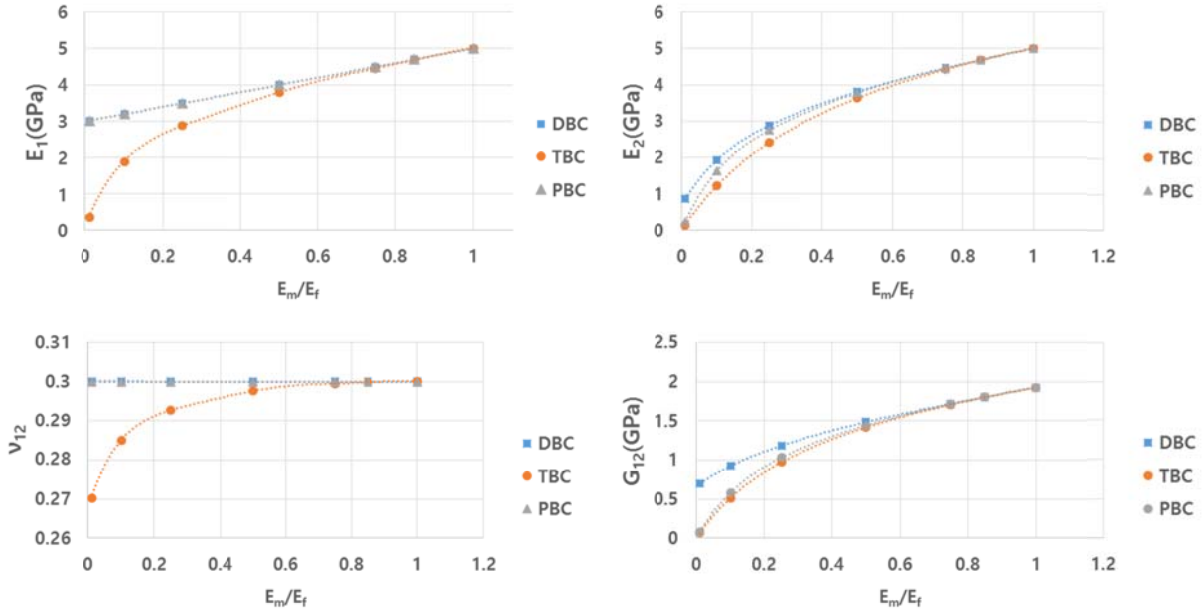

Fig. 1 Effects of boundary conditions and stiffness contrast of constituents to the effective stiffnesses

5.2 Effects of Spatial Random Distributions of Matrix Properties

To scrutinize the effects of random distribution of constituents' property, statistical analysis was performed by sampling multiple realizations of random distribution of Young's modulus of matrix. For the realizations, $\sigma_{\mathrm{LN}} = 0.25$ GPa, $< E > = 2.5$GPa and correlation length $L_x = 40\mu m, L_y = L_z = 8\mu m$ were assumed. Fig. 2 shows that effective stiffnesses (i.e. E_1 and E_2) show corresponding statistical variations with 400 samples. For normalized longitudinal Young's modulus, $<E_1/E_m>$=1.597, σ_{E_1/E_m} =0.0260. For transverse directional Young's modulus, $<E_2/E_m>$=1.5079 $\sigma_{E_2/\mathrm{E_m}}$=0.0411. Interestingly, E_2 variation was more significant than E_1 because of the short correlation length in y and z directions.

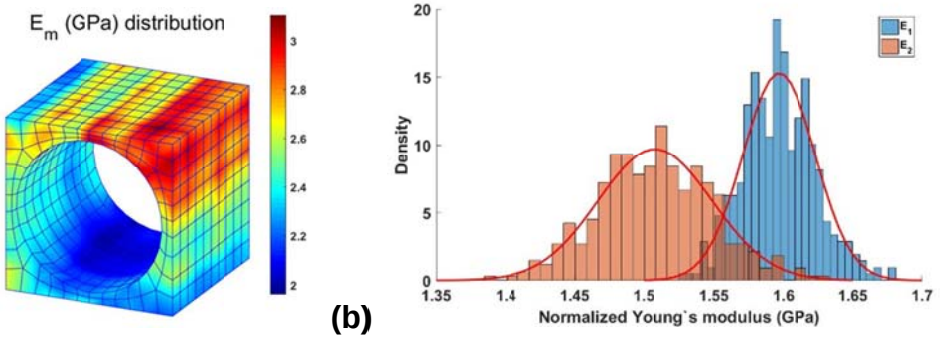

Fig.2 (a) a sample of random distribution of matrix Young's modulus and (b) histograms of normalized effective stiffness

6. CONCLUSIONS

In this study, effects of boundary conditions to the effective stiffnesses of heterogeneous RVE were investigated by computational homogenization technique for multiscale analysis. Heterogeneity was introduced by varying stiffness contrast and spatial random distributions of matrix properties. Certainly, differences of the effective stiffnesses for boundary conditions increases as the level of stiffness contrast increases. Moreover, it was observed that the random distributions of matrix properties can also significantly change the effective stiffnesses.

ACKNOWLEDGMENTS

This work was supported by Creative-Pioneering Researchers Program through Seoul National University (SNU). Authors are grateful for their supports.

REFERENCES

Benssousan, A., J. L. Lions and G. Papanicolaou (1978). Asymptotic Analysis for Periodic Structures. Amsterdam, North Holland.
Dvorak, G. J. and Y. A. Baheieldin (1982). "Plasticity Analysis of Fibrous Composites." Journal of Applied Mechanics-Transactions of the Asme **49**(2): 327-335.
Eshelby, J. D. (1957). "The Determination of the Elastic Field of an Ellipsoidal Inclusion, and Related Problems." Proceedings of the Royal Society of London Series a-Mathematical and Physical Sciences **241**(1226): 376-396.
Hashin, Z. and S. Shtrikman (1963). "A Variational Approach to the Theory of the Elastic Behaviour of Multiphase Materials." Journal of the Mechanics and Physics of Solids **11**(2): 127-140.
Hill, R. (1965). "A Self-Consistent Mechanics of Composite Materials." Journal of the Mechanics and Physics of Solids **13**(4): 213-&.

Hollister, S. J. and N. Kikuehi (1992). "A comparison of homogenization and standard mechanics analyses for periodic porous composites." Computational Mechanics **10**: 73-95
Kaminski, M. and A. Pawlak (2015). "Various approaches in probabilistic homogenization of the CFRP composites." Composite Structures **133**: 425-437.
Mori, T. and K. Tanaka (1973). "Average Stress in Matrix and Average Elastic Energy of Materials with Misfitting Inclusions." Acta Metallurgica **21**(5): 571-574.
Nguyen, V. P., M. Stroeven and L. J. Sluys (2011). "Multiscale Continuous and Discontinuous Modeling of Heterogeneous Materials: A Review On Recent Developments." Journal of Multiscale Modelling **3**(4): 229–270.
Ostoja-Starzewski, M. (2008). Microstructural Randomness and Scaling in Mechanics of Materials. BOca Raton, Florida, Taylor &Francis Group, LLC.
Ozdemir, I., W. A. M. Brekelmans and M. G. D. Geers (2008). "FE2 computational homogenization for the thermo-mechanical analysis of heterogeneous solids." Computer Methods in Applied Mechanics and Engineering **198**(3-4): 602-613.
Salnikov, V., S. Lemaitre, D. Choi and P. Karamian-Surville (2015). "Measure of combined effects of morphological parameters of inclusions within composite materials via stochastic homogenization to determine effective mechanical properties." Composite Structures **129**: 122-131.
Spanos, P. D. and A. Kontsos (2008). "A multiscale Monte Carlo finite element method for determining mechanical properties of polymer nanocomposites." Probabilistic Engineering Mechanics **23**(4): 456-470.
Stefanou, G., D. Savvas and M. Papadrakakis (2015). "Stochastic finite element analysis of composite structures based on material microstructure." Composite Structures **132**: 384-392.
Sun, C. T. and R. S. Vaidya (1996). "Prediction of composite properties, from a representative volume element." Composites Science and Technology **56**(2): 171-179.
Terada, K., M. Hori, T. Kyoya and N. Kikuchi (2000). "Simulation of the multi-scale convergence in computational homogenization approaches." International Journal of Solids and Structures **37**(16): 2285-2311.
Yuan, Z. and J. Fish (2008). "Toward realization of computational homogenization in practice." International Journal for Numerical Methods in Engineering **73**(3): 361-380.
Zhou, X. Y., P. D. Gosling, C. J. Pearce, L. Kaczmarczyk and Z. Ullah (2016). "Perturbation-based stochastic multi-scale computational homogenization method for the determination of the effective properties of composite materials with random properties." Computer Methods in Applied Mechanics and Engineering **300**: 84-105.
Zhu, H., Q. Wang and X. Zhuang "A nonlinear semi-concurrent multiscale method for dynamic fractures." International Journal of Impact Engineering **87**: 65-82.
Zhuang, X. Y., Q. Wang and H. H. Zhu (2015). "A 3D computational homogenization model for porous material and parameters identification." Computational Materials Science **96**: 536-548.